Ion-irradiation effects on the phonon correlation length of graphite studied by Raman spectroscopy

Kazutaka Nakamura and Masahiro Kitajima
Second Research Group, Tsukuba Laboratories, National Research Institute for Metals, 1-2-1 Sengen, Tsukuba-shi, Ibaraki-ken 305, Japan
(Received 1 May 1991)

Real-time Raman measurements have been performed on graphite under 3-keV Ar^+-ion irradiation with a time resolution of 6 sec. Ion flux of 3×10^{11} and 4×10^{10} ions/cm^2 sec are used. The graphite lattice damage is estimated by the relative intensity ratio of the disorder-induced peak (~1360 cm^{-1}) with respect to the Raman-active E_{2g}-mode peak (~1580 cm^{-1}). The relative intensity change in the Raman spectrum caused by the irradiation is explained in terms of a reduction in the phonon correlation length due to defects.

I. INTRODUCTION

In spite of a large number of Raman studies on carbon materials irradiated with energetic ions for characterizing microscopic structural properties, the Raman scattering of graphite lattice disorder in the early stage of irradiation has yet to be well established. In this paper we present a measurement on the time dependence of Raman scattering of graphite under ion irradiation with low energy and flux in an ultrahigh vacuum chamber to study the initial change of Raman scattering by the lattice disorder.

Ion-implanted materials, such as III-V semiconductors and carbon materials, have been extensively studied by Raman spectroscopy since Raman scattering is sensitive to a state of material and ion implantation usually takes place within an optical skin depth. Tiong *et al.*[1] studied Raman scattering of As^+-ion-implanted GaAs and found that defects, and not only crystallite size, cause systematic changes in the LO-phonon line shape. They explained the LO phonon line shape and positions in terms of the spatial correlation model and suggested that the phonon correlation length, an average size of the undamaged regions, could be obtained from Raman spectra.

Since the measurement by Smith *et al.*[2] on graphite irradiated with Ar ions, graphite irradiated with various ions has been studied by Raman spectroscopy in connection with studies on graphite intercalation compounds[3–5] and on plasma wall interaction in a fusion device.[6,7] Raman scattering of graphite is sensitive to its structural disorder. While single-crystal graphite exhibits a sharp line of Raman-active E_{2g}-mode lattice vibration at around 1580 cm^{-1}, poorly ordered graphite materials, such as glassy carbon or charcoal, exhibit an additional disorder-induced line at around 1360 cm^{-1} where the phonon density of states has a strong maximum. It is well known that the relative intensity of the disorder-induced line with respect to the Raman-active E_{2g} mode line is inversely proportional to an in-plane microcrystallite size (L_a).[8,9] Previous studies[10,11] of the Raman scattering on the electron beam irradiated graphite showed that line positions of Raman-active E_{2g} mode were explained in terms of the phonon dispersion and the wave vector uncertainty derived from the L_a and suggested that the L_a corresponds to the phonon correlation length.

Cascade process caused by the ion irradiation produces a disorder region around an ion trajectory, and the Raman spectrum exhibits a double-peaked spectrum. The relative intensity between two peaks varies as a degree of disorder. At a sufficiently high dosage, an amorphous layer is formed and the Raman spectrum exhibits a broad asymmetric line at around 1500 cm^{-1}. Elman *et al.*[3,4] studied Raman scattering of crystallite graphite implanted with ^{11}B ions at a fluence in the 1×10^{14} to 2.5×10^{16} ions/cm^2 range and energy of 100 keV and found that abrupt transformation to an amorphous structure occurred at 5×10^{15}. The spectrum for the sample implanted at a fluence of 1×10^{14} ions/cm^2 already exhibited a long-range disordered feature before the amorphous transformation.

In the present study, real-time Raman measurements have been performed and attention is focused on the initial change in the Raman spectrum caused by the low energy ion irradiation. Real-time measurements can provide direct information on kinetics of lattice damage under irradiation. We discussed on the relation between spatial correlation of phonon and a mean distance between defects caused by ion irradiation. The relation between the observed Raman spectrum and the depth profile of lattice damage is also discussed.

II. EXPERIMENT

The sample used was a highly oriented pyrolytic graphite (HOPG, grade ZYA from Union Carbide), with its size being $12\times12\times2$ mm^3. The sample was cleaved using the adhesive tape technique for each measurement. The ion irradiation was performed in a ultrahigh vacuum chamber (base pressure $<10^{-8}$ Pa) with an energy of 3 keV. The incident angle of the ion beam was 45 degrees normal to the c face. Ion flux of 3×10^{11} and 4×10^{10} ions/cm^2 sec were examined. Incident radiation of 514.5 nm and 500 mW was provided using a cw argon-ion laser

(Coherent Radiation Model INNOVA 70). The scattered radiation was collected through the sapphire window of the chamber in back-scattering configuration, analyzed by a double-grating monochrometer (Japan Spectroscopic Company Ltd., TRS-660), and detected by a spectrometric multichannel analyzer (Princeton Instruments Inc., IRY-700). The spectrometric multichannel analyzer has 700 channels and detects to a width of about 400 cm^{-1}. The minimum exposure time of the detector is 33 msec, and the exposure time used for the experiment was 180 times the minimum exposure time (about 6 sec) to get intense signals. Ion irradiation was performed over 250 sec and Raman spectrum was measured at about 6 sec intervals. The sample temperature was monitored by a chromel-almel thermocouple held in contact with the sample and mount. The temperature increased to $\sim 60\,^{\circ}C$ by the laser annealing effect, but the Raman spectrum did not change due to the temperature increase. Details of the experimental setup are described elsewhere.[12] Raman spectra were analyzed with numerical decomposition by assuming the Lorentzian line shape for the peaks.

III. RESULTS AND DISCUSSION

Figure 1(a) shows a typical example of a first-order Raman spectrum of HOPG before Ar^+ ion irradiation. The peak observed at $\sim 1580\ cm^{-1}$ (G) is a Raman active E_{2g} mode vibration peak. Ion irradiation induced a peak at $\sim 1360\ cm^{-1}$ (D) as shown in Figs. 1(b)–1(e) which were measured during ion irradiation at 18, 48, 78, and 108 sec after the beginning of the irradiation at a flux of 3×10^{11} ions/cm^2 sec. The disorder induced peak D was attributed to a maximum of the density of state of phonon. The solid curves are the results of computer simulation obtained by assuming the Lorentzian line shape. The peak height of D peak increases and that of G peak decreases with an increase in the irradiation time as shown in Fig. 2. The line width of both D and G peaks, on the other hand, increase by irradiation as shown in Fig. 3. A drastic change in line width and intensity and a broad asymmetric Raman line centered at about 1500 cm^{-1}, characteristic of the amorphous regime, were not observed. The line width of D peak is more sensitive to the lattice disorder than that of G peak. The in-plane phonon correlation length can be deduced from peak intensity ratio (R) of the D peak with respect to the G peak[8,9] by use of the formula $L_a = 4.4/R$ (nm). R is then a measure of the disorder caused by the lattice damage, and plotted as a function of irradiation time in Fig. 4. The ion irradiation at lower flux of 4×10^{10} ions/cm^2 sec was also performed and the increase in the D peak was slower than that for the irradiation at a flux of 3×10^{11} ions/cm^2 sec (Fig. 6).

Since the optical skin depth is larger than the penetration depth of implanted particles, the observed Raman spectrum is made up by the superposition of scattering from both damaged and nondamaged layers. For example, Ishida *et al.*[13] studied 2-keV Ar^+ etched HOPG by surface enhanced Raman scattering (SERS), which provides information of the outer most surface, and showed that the damage estimated from a SERS spectrum is much stronger than that from a usual Raman spectrum.

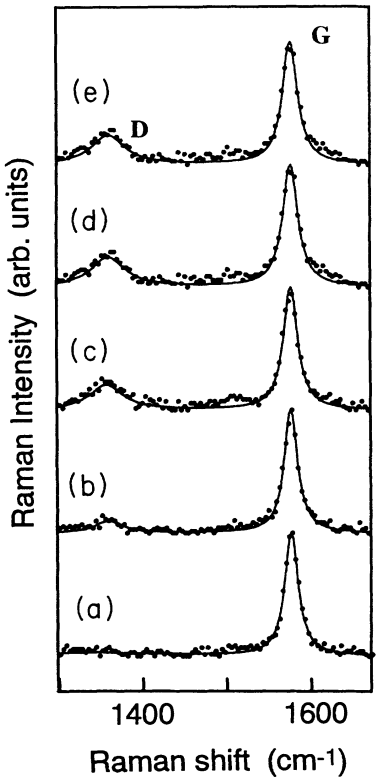

FIG. 1. Raman spectra of HOPG (a) before ion irradiation, and obtained during the irradiation after (b) 18, (c) 48, (d) 78, and (e) 108 sec from the beginning of the irradiation of 3-keV Ar^+ at a flux of 3×10^{11} ions/cm^2 sec. Solid curves are the computer simulation results. The peak at $\sim 1580\ cm^{-1}$ (G) is a Raman active E_{2g} mode peak and the peak at $\sim 1360\ cm^{-1}$ (D) is a disorder-induced peak.

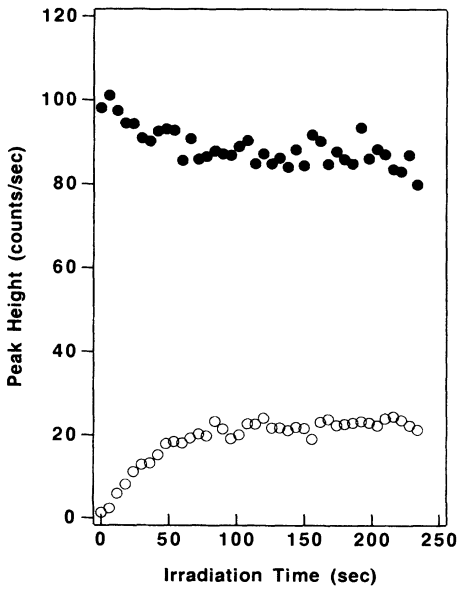

FIG. 2. Time dependence of the peak height of HOPG for the irradiation of 3-keV Ar^+ at a flux of 3×10^{11} ions/cm^2 sec, the disorder-induced line (○) and the Raman active line (●).

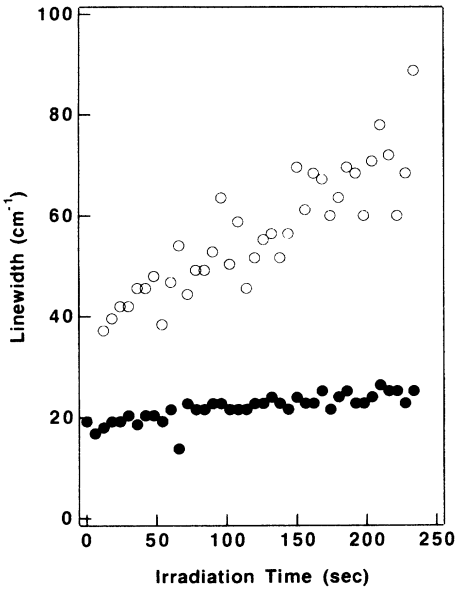

FIG. 3. Time dependence of the linewidth for the irradiation of 3-keV Ar^+ at a flux of 3×10^{11} ions/cm^2 sec, the disorder-induced line (○) and the Raman active line (●).

It is then important to estimate contribution from damaged layers to study the actual ion irradiation effects.

We calculated profiles of implanted particles and energy deposition using the Monte Carlo method (TRIM85 code[14]). Figure 5 shows results of the calculation on the 3-keV ion irradiation with an angle of 45 degrees to c face. While the implanted particles are distributed at an average penetration depth of 3 nm, the nuclear energy deposition occurred near the surface. The distribution of the nuclear energy deposition [$F(x)$ for the depth of x] can be approximated by the Gaussian function with the standard deviation of 1.5 nm. The average number of vacancies was estimated to be 16 per implanted ion from the energy deposition and larger than the number of implanted particles. A distribution profile of the lattice damage induced by the ion irradiation may correspond to that of the nuclear energy deposition. The effects from displaced carbon atoms to the relative peak intensity for in-plane lattice vibration may be weak, since they are trapped between graphite layers. Recently, Holtz *et al.*[16] studied the Raman scattering depth profile of the structure of 45-keV Be^+ ion-implanted GaAs with chemical-etch removal of surface layers and found that the structural depth profile of the damage layer derived from Raman spectra agreed with that estimated from TRIM calculation. Since the lattice damage is characterized by the peak intensity ratio, the intensity ratio [$R(x)$] of the Raman spectrum from the layer at depth of x can be ex-

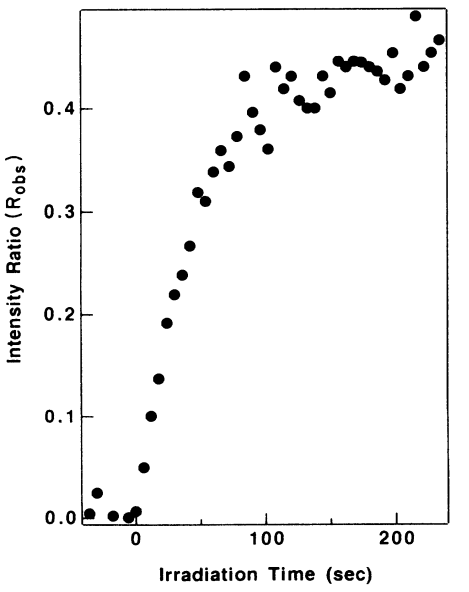

FIG. 4. Time dependence of the relative intensity ratio of the disorder-induced line with respect to the Raman active line for the irradiation of 3-keV Ar^+ at a flux of 3×10^{11} ions/cm^2 sec.

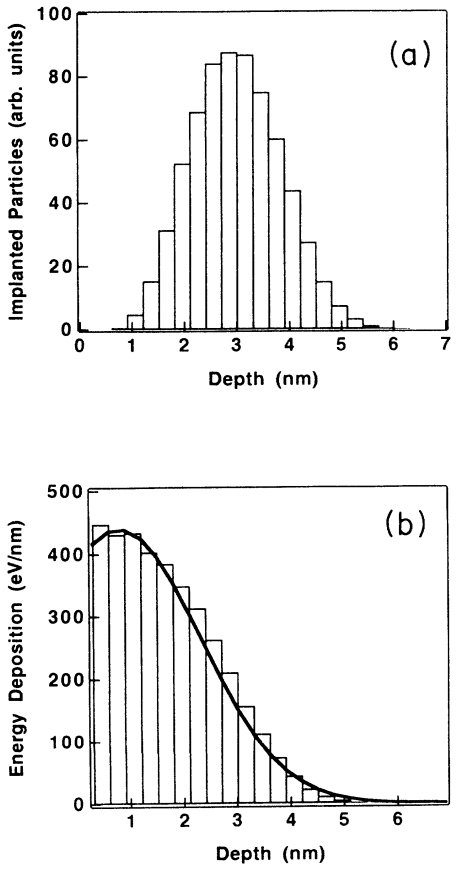

FIG. 5. Distribution profiles of implanted particles and nuclear energy deposition calculated by the Monte Carlo method for the 3-keV Ar^+ irradiation with the angle of 45 degrees to the graphite c face; (a) implanted particles, (b) nuclear energy deposition, the solid curve is the best fit with the Gaussian function of centered at 0.8 nm and the standard deviation of 1.5 nm.

pressed by

$$R(x)=R_0PF(x)\ , \tag{1}$$

where the R_0 is the mean value of the relative intensity ratio within the whole range of energy deposition ($P=5$ nm) and the area of $F(x)$ is normalized to unity.

Since the incident and scattered light are absorbed by graphite, detectable Raman scattering intensity $I(x)$ for both G and D from the layer at the depth of x is expressed by

$$I(x)=I_0\exp(-8\pi kx/\lambda)\ , \tag{2}$$

where λ is the wavelength of the exciting light, I_0 is the proportionality constant, and k is the optical parameter ($k=0.9$ for carbon material).[13,15] Observed peak intensity ratio $R_{\rm obs}$ is then calculated by

$$R_{\rm obs}=\frac{\int_0^\infty R(x)I(x)dx}{\int_0^\infty I(x)dx}\ . \tag{3}$$

For the case of the 3-keV Ar^+ irradiation $R_{\rm obs}$ is calculated to be $\sim 0.2\ R_0$. The corrected intensity ratio for the ion irradiation at the flux of 3×10^{11} ions/cm^2 sec and 4×10^{10} ions/cm^2 sec are shown in Fig. 6.

Previous Raman studies[3,4] on high-temperature annealing of ^{11}B ion implanted graphite showed that annealing at a temperature as low as 700 °C caused a decrease in the relative intensity of D peak to G peak and in the linewidth by a restoration of the structural order. This annealing temperature, however, is lower than the temperature of graphitization. The in-plane ordering takes place between 1300 °C and 1500 °C and three-dimensional ordering takes place above 2000 °C.[4] Therefore, the restoration of the structural order may be due to diffusion of the defects and the defects may dominate the structural disorder induced.

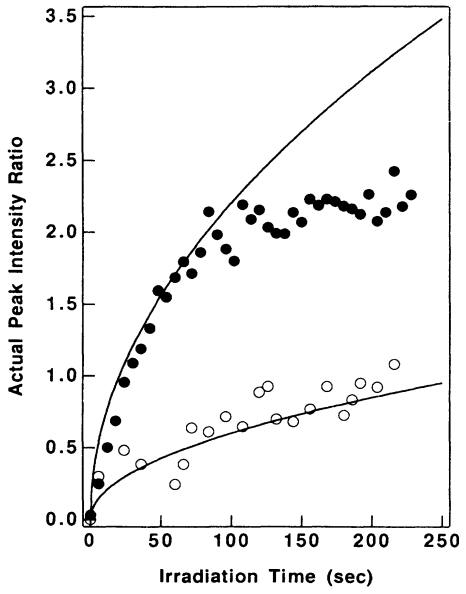

FIG. 6. Time dependence of the actual intensity ratio for the irradiation of 3-keV Ar^+ at flux of 4×10^{10} ions/cm^2 sec (○) and 3×10^{11} ions/cm^2 sec (●). Solid curves are results of calculation with Eq. (7).

In general, the number of defects (N_d) per unit volume induced by ion irradiation is given by

$$N_d=N\sigma\varphi\nu t\ , \tag{4}$$

where N is the density of target (1.25×10^{23} atoms/cm^3), σ is the displacement cross section, φ is the incident ion flux, ν is the mean number of displaced atoms in the cascade per primary knock-on, and t is the irradiation time.[17] Since graphite has a layer structure, the mean number of defects per layer (N_L) is

$$N_L=fN_d\ , \tag{5}$$

where f is the distance between the graphite layers (0.335 nm). The mean distance (L) between in-plane defects can be given by

$$L=\frac{1}{\sqrt{N_L}}\ . \tag{6}$$

We assumed that L corresponds to in-plane phonon correlation length L_a because the defect may cut or change the interaction between lattice atoms. The mean relative intensity ratio of the Raman peaks within the ion penetration depth is then expressed by

$$R=4.4\times10^{-7}\sqrt{fN\sigma\varphi\nu}\sqrt{t}\ , \tag{7}$$

and proportional to the square root of the irradiation time.

In the present case of 3-keV Ar^+ irradiated graphite, the reduced energy ε is 0.072. For $\varepsilon<0.2$, the displacement cross section is calculated by the Sigmund theory[18,19] by

$$\sigma=1.9635a^2(m_1/m_2)^{1/3}(2z_1z_2e^2/a)^{2/3}\times E_0^{-1/3}(E_d^{-1/3}-T_{\rm max}^{-1/3})\ , \tag{8}$$

where a is the screening radius, E_0 the incident ion energy, $T_{\rm max}$ the maximum of the transferred energy, e the electronic charge, E_d the threshold energy for displacement, m_1, z_1, m_2, and z_2, the mass and atomic numbers of the projectile and target, respectively. The total displaced atoms (ν) can be calculated by a simplified model of the Kinchin-Pease theory,[20,21]

$$\nu=0.5\{1+\ln(T_{\rm max}/2E_d)\}\ . \tag{9}$$

Using the displacement threshold energy of 29.7 eV obtained by the etch-decoration technique,[22] we obtained the values of 2.3 and 9.5×10^{-17} cm^2 for ν and σ, respectively. Calculated relative intensity by Eq. (7) is shown in Fig. 6 and agrees well with experimental data for both flux 3×10^{11} ions/cm^2 sec and 4×10^{10} ions/cm^2 sec. Our simplified calculation suggests that the in-plane phonon correlation length is in agreement with the mean distance between defects in graphite plane in the lower fluence range. This is reasonable because defects or vacancies induced by the ion-irradiation change interaction around

them and cut the long-range phonon interaction.

A considerable reason for the deviation between calculation and experiments after 150 sec for the flux of 3×10^{11} ions/cm^2 sec is the creation of the defect clusters. If defects aggregate and create clusters, the effective distance between defects or clusters increases. For the neutron irradiation experiments, the creation of defect clusters at a high flux range was suggested from the change in the thermal and electrical conductivities.[23] Another possible reason is the breakdown in the relation between Raman intensity ratio (I_D/I_G) and the phonon correlation length for $L_a < 2.5$ nm.[8]

In conclusion, real-time *in situ* Raman measurements were performed on a graphite lattice to assess the damage caused by Ar^+ irradiation. Change in the Raman spectrum of graphite in early stages of the irradiation is explained in terms of a reduction in the phonon correlation length due to defects.

[1]K. K. Tiong, P. M. Amirtharaj, F. H. Pollak, and D. E. Aspnes, Appl. Phys. Lett. **44**, 122 (1984).
[2]J. E. Smith, Jr., M. H. Brodsky, B. L. Crowder, and M. I. Nathan, J. Non-Cryst. Solids **8-10**, 179 (1972).
[3]B. S. Elman, M. Shayegan, M. S. Dresselhaus, H. Mazurek, and G. Dresselhaus, Phys. Rev. B **25**, 4142 (1982).
[4]B. S. Elman, M. S. Dresselhaus, G. Dresselhaus, E. W. Maby, and H. Mazurek, Phys. Rev. B **24**, 1027 (1981).
[5]M. S. Dresselhaus and G. Dresselhaus, in *Light Scattering in Solid III,* edited by M. Cardona and G. Güntherodt (Springer-Verlag, Berlin, 1982), p. 2.
[6]M. Kitajima, K. Aoki, and M. Okada, J. Nucl. Mater. **149**, 269 (1987).
[7]T. Tanabe, S. Muto, Y. Gotoh, and K. Niwase, J. Nucl. Mater. **175**, 258 (1990).
[8]D. S. Knight and W. B. White, J. Mater. Res. **4**, 385 (1989).
[9]F. Tuinstra and J. L. Koenig, J. Chem. Phys. **53**, 1126 (1970).
[10]K. Nakamura, M. Fujitsuka, and M. Kitajima, Phys. Rev. B **41**, 12 260 (1990).
[11]K. Nakamura, M. Fujitsuka, and M. Kitajima, Chem. Phys. Lett. **172**, 205 (1990).
[12]K. Nakamura and M. Kitajima, Appl. Phys. Lett. **59**, 1550 (1991).
[13]H. Ishida, H. Fukuda, G. Katagiri, and A. Ishitani, Appl. Spectros. **40**, 322 (1986).
[14]J. F. Ziegler, J. P. Biersack, and U. Littmark, in *The Stopping and Range of Ions in Solids* (Pregamon, New York, 1985), p. 109.
[15]D. L. Greenaway and G. H. Harbeke, Phys. Rev. **178**, 1340 (1969).
[16]M. Holtz, R. Zallen, O. Brafman, and S. Matteson, Phys. Rev. B **37**, 4609 (1988).
[17]F. Seitz and J. S. Koehler, in *Solids State Physics* **2**, 305 (1956).
[18]P. D. Townsend, J. C. Kelly, and N. E. W. Hartley, in *Ion Implantation, Sputtering and their Applications* (Academic, London, 1976), p. 117.
[19]P. Sigmund, in *Sputtering by Particle Bombardment I,* edited by R. Behrisch (Springer-Verlag, Berlin, 1981), p. 9.
[20]Y. Kido and H. Nakano, Surf. Sci. **239**, 254 (1990).
[21]G. H. Kinchin and R. S. Pease, Rep. Prog. Phys. **18**, 1 (1955).
[22]G. L. Montet, Carbon **11**, 89 (1973).
[23]B. T. Kelly, Carbon **20**, 3 (1982).